Li adsorption versus graphene intercalation on Ir(111): From quenching to restoration of the Ir surface state

P. Pervan,[1,*] P. Lazić,[2,4,†] M. Petrović,[1] I. Šrut Rakić,[1] I. Pletikosić,[1] M. Kralj,[1,4] M. Milun,[1] and T. Valla[3]

[1]*Institut za fiziku, Bijenička 46, HR-10000, Zagreb, Croatia,*

[2]*Institut Ruđer Bošković, Bijenička 54, 10000, Zagreb, Croatia,*

[3]*Department of Condensed Matter Physics & Materials Science, Brookhaven National Laboratory, Upton, New York 11973, USA*

[4]*Center of Excellence for Advanced Materials and Sensing Devices, Bijenička 46, HR-10000, Zagreb, Croatia*

(Received 20 August 2015; revised manuscript received 12 November 2015; published 10 December 2015)

It is common knowledge that even a trace amount of a chemisorbed species can strongly perturb the surface electronic structure, in particular the surface states, to the point of their complete eradication. We have confirmed this behavior by adsorbing Li on the Ir(111), but surprisingly, we have discovered that in the presence of graphene Li does not suppress the Ir surface state. By combining the results of the low-energy electron diffraction and angle-resolved photoemission spectroscopy with the density functional theory for modeling of the studied systems we can provide a detailed explanation for the observed phenomena. The quenching of the surface state by the electronic states of disordered Li layer on a bare Ir surface is efficiently deactivated by the presence of graphene which shifts the Li states to lower energies thereby leading to the unexpected reappearance of the surface state. Such protection of the surface state coherence from disorder upon intercalation could be used as a benchmark in the toolbox of surface science.

DOI: 10.1103/PhysRevB.92.245415 PACS number(s): 68.65.Pq, 71.15.Mb, 73.20.At, 73.22.Pr

I. INTRODUCTION

Surface states (SS) appear as electron states (bands) highly localized perpendicular to the plane of low index surfaces of metals and semiconductors. They play an important role in many physical processes taking place at surfaces (e.g., catalytic reactions) and material interfaces (e.g., Schottky barriers). Due to their atomic scale localization in the surface region they are extremely sensitive to the presence of adsorbates [1]. A convincing example of the response of surface states to chemisorbed species was revealed in the angle-resolved photoemission spectroscopy (ARPES) observations of the Shockley SS on Cu(001) which were fully removed from the spectrum upon oxygen exposure [2]. However, adsorption may also have a more subtle influence on the SS. Alkali metals (AM) are known to induce a shift of the SS to higher binding energies [3–5], accompanied by the broadening of SS peak as a signature of reduced momentum coherence [6]. Generally, adsorbates can generate a wide spectrum of changes in the SS properties [7,8]. Yet, surfaces covered with a graphene layer may show a very different interaction with adsorbates with respect to the bare surface. For Ir(111) SS it has been experimentally demonstrated that graphene protects it from adsorbates even when the sample is exposed to ambient pressure [9]. Conversely, it is expected that intercalated atoms, chemisorbed randomly between graphene and the substrate, would interact with the underlying surface in a manner similar to the bare surface, leading to quenching of the SS. Such a behavior was demonstrated in the case of intercalated oxygen [10]. It is far less intuitive that physisorbed graphene may have any significant impact on the interaction of intercalated species chemisorbed on the underlying surface such that the surface state remains coherent for any configuration of the adsorbent. This leeds us to the different scenario of intercalated graphene to surface intercations: not only that intercalated atoms can decouple graphene from the substrate but graphene can, to a certain extent, decouple intercalant from the substrate surface.

II. EXPERIMENTAL AND COMPUTATIONAL DETAILS

Experiments have been performed in an ultra-high vacuum (UHV) ARPES facility in Zagreb and at the ANTARES station at the Soleil synchrotron [the first preliminary results were obtained on the U13 station at the National Synchrotron Light Source (NSLS) of Brookhaven National Laboratory]. An iridium single crystal of the 99.99% purity and orientation accuracy better than 0.1° was used. The substrate was cleaned by several cycles of sputtering with 1.5 keV Ar^+ ions at room temperature or elevated temperature (1100 K) followed by annealing at 1500–1600 K. The cleanliness and quality of Ir(111) were checked by low-electron energy diffraction (LEED) and ARPES (SS sharpness and intensity). The graphene monolayer on Ir(111) was prepared by a temperature programmed growth cycle (TPG, room temperature ethene exposure 6×10^{-6} Pa for 60 seconds and flash to 1400 K) followed by a chemical vapor deposition (CVD, 6×10^{-6} Pa of ethene for 300 s while the sample held at 1150 K) [11]. This TPG + CVD procedure growth leads to uniform orientation of graphene [refered to as Gr/Ir(111)] with the lattice aligned to the substrate lattice (R0) and at full monolayer coverage [11]. Lithium was deposited from a commercial getter source while the sample surface was kept at room temperature.

The ARPES spectra were recorded by the Scienta SES 100 hemispherical electron analyzer with an overall energy resolution of 25 meV and an angular resolution of 0.2°. Photons of 21.2 eV from a nonpolarized He discharge ultraviolet source (beam spot diameter of around 2 mm) were used for excitation. The sample was cooled to 60 K during the ARPES spectra acquisition.

Ab initio calculations were performed within the framework of density functional theory (DFT) as implemented in the VASP code with the projector augmented wave (PAW) method.

*pervan@ifs.hr,
†plazic@irb.hr

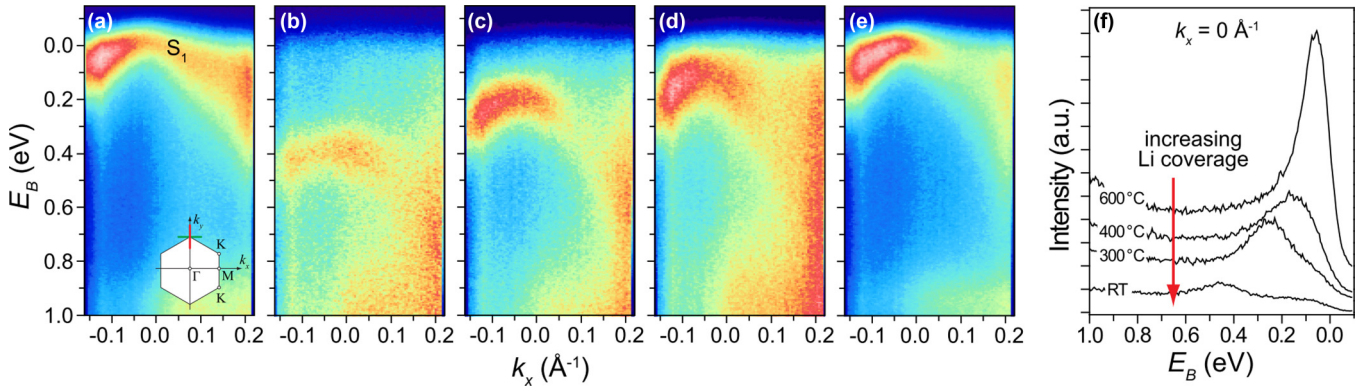

FIG. 1. (Color online) Photoemission spectra of Ir surface state S_1 around the K point along k_x direction in the SBZ (see the inset) (a) bare Ir(111), (b) Ir(111) saturated by Li at RT and subsequently annealed at (c) 300 °C, (d) 400 °C, (e) 600 °C. (f) The corresponding EDC of the Ir surface state S_1 taken at $k_x = 0\,\text{Å}^{-1}$.

We used self-consistently implemented van der Waals density functional (vdW-DF) [12] for correlation in combination with the optB88 exchange. The lattice constant of Ir bulk was determined self-consistently while the graphene lattice constant was adjusted to match the Ir(111) surface lattice constant resulting in some strain on the graphene. In all calculations the expansion in plane waves was done using the cutoff energy of 500 eV. The Brillouin zone was sampled by a Monkhorst-Pack [13] choice of k points, namely $15 \times 15 \times 1$, $9 \times 9 \times 1$, $5 \times 5 \times 1$, and $3 \times 3 \times 1$ points were used for the unit cell sizes 1×1, 2×2, 3×3, and 4×4, respectively. The Ir(111) surface slab was simulated by five atomic layers of which the top two, along with the C and Li atoms, were allowed to relax until the forces on atoms were below 1 meV/Å. Dipole correction [14] in the direction perpendicular to the slab was used with 20 Å of vacuum separating the periodic slab images.

Unfolding of the band structure for the unit cells larger than 1×1 was done using the theory from Ref. [15] as implemented in the BANDUP code [16]. Charge density differences were obtained by calculating the charge differences between the system (Ir-Li-Gr) and system parts as positioned in the system. In all configurations the optimal energy is achieved with the Li atom in the hcp position with respect to the Ir(111) surface, and with C atoms in on-top and fcc positions (a nonlocal binding energy distribution was analyzed using the JUNOLO code) [17].

III. EXPERIMENTAL RESULTS AND DISCUSSION

In this work we combined the experimental (LEED and ARPES) and theoretical methods (DFT) to investigate the interaction of Ir SS with adsorbed Li [referred to as Li/Ir(111)] and the modification introduced by graphene positioned on top of Li/Ir(111). Specifically, it has been shown that Ir(111) supports three SS close to the K point [18] of the surface Brillouin zone (SBZ). The one at the Fermi level, exhibiting the d_{z2} symmetry (S_1), is in the focus of the present study. The formation of graphene on the Ir surface strongly reduces the spectral intensity of the S_1 surface state, when probed with 21.2-eV photons (see Fig. 2 in Ref. [11]). Starodub *et al.* [19] reported a strong hybridization of this Ir state with graphene π bands.

We first investigated the interaction of the S_1 state on the bare Ir surface with adsorbed Li atoms. LEED measurements show that Li/Ir(111) does not exhibit ordered structures for any concentration of Li. Figure 1(a) shows the ARPES spectra around the K point parallel to the Γ-M-Γ direction (k_x, see the inset) of the bare Ir(111) with the S_1 state at the Fermi level clearly discernible. A series of ARPES spectra shown in Figs. 1(b) to 1(e) are related to Ir(111) saturated by Li [we refer to this system as one monolayer (ML) Li/Ir(111)] and subsequently annealed at increasing temperatures, leading to a reduction of the Li coverage. By comparing Figs. 1(a) and 1(b) it is obvious that Li monolayer induces a strong shift of the S_1 state to higher binding energy (0.43 eV) and at the same time substantially reduces its intensity. Figure 1(f) shows the corresponding energy distribution curves (EDCs) that exhibit the expected response of SS to AM adsorption; the increase of Li coverage and a shift of the SS away from the Fermi level are accompanied by a strong reduction of the spectral intensity. Next, we investigated the Li covered Ir(111) overlaid with graphene (Gr) referred to as Gr/Li/Ir(111). Such a structure is obtained by Li intercalation of the Gr/Ir(111) system. To date, numerous aspects of Li intercalation of graphene have been studied experimentally [20–24] and theoretically [25–28], confirming that Li intercalates graphene at room temperature [20]. Bare and fully intercalated Gr/Ir(111) were characterized by ARPES [29]. The main features of the intercalated system are as follows: nearly linearly dispersing graphene π bands, π bands renormalization around the Fermi level due to electron phonon coupling, and a strong shift of the Dirac point (1.63 eV) characteristic of the AM intercalation [30]. Figures 2(a) to 2(e) show a set of ARPES spectra of Gr/Ir(111) intercalated by an increasing amount of Li with the main additional feature: the shift of the S_1 state (0.43 eV) below the Fermi level. It is worth mentioning that under the same experimental conditions the well-known Rashba split SS in the Ir zone center Γ shifts to higher binding energy and quickly disappears from the spectrum as it hybridizes with the bulk bands. A similar shift of the S_1 state has been previously observed in Gr/Ir(111) intercalated by ordered monolayers of Cu [31] and Pt [32]. The corresponding LEED patterns obtained at various Li concentrations [Figs. 2(f) to 2(h)] show that only at saturation coverage does Li exhibit an ordered phase. Namely, Li intercalation is accompanied by a continuous decrease of the Ir and moiré diffraction spots [see Fig. 2(g)], leaving only the graphene spots clearly visible,

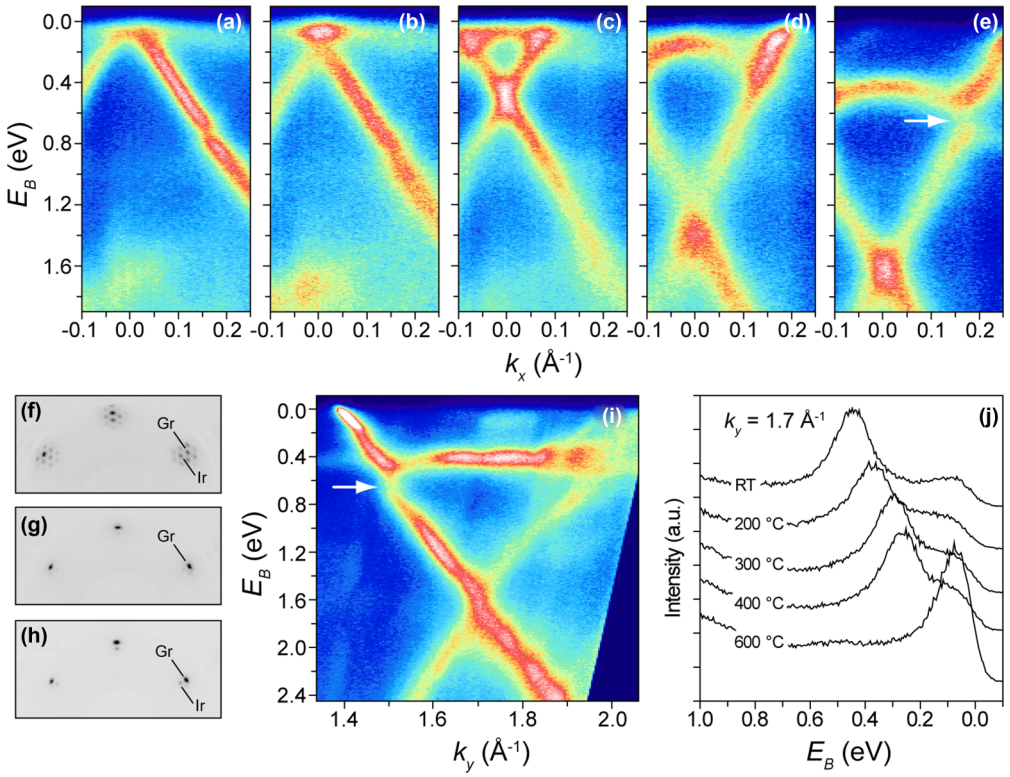

FIG. 2. (Color online) (a)-(e) Photoemission spectra around the K point of BZ along k_x for different concentrations of Li deposited at RT. (f) LEED pattern of Gr/Ir(111) with Ir and graphene spots and additional spots corresponding to moiré superstructure. (g) LEED pattern of Gr on Ir intercalated by Li. (h) LEED pattern of Gr/Li(1 × 1)/Ir(111) (see text). All three LEED patterns were obtained with electrons of kinetic energy equal to 69 eV. (i) Same as (e) but taken along k_y. Spectra (e) and (i) correspond to Gr/Li(1 × 1)/Ir(111), (j) EDC of the S_1 taken at $k_y = 1.7\,\text{Å}^{-1}$ from Gr/Li(1 × 1)/Ir(111) during Li de-intercalation obtained by annealing the sample at different temperatures as indicated.

and indicating the lack of order in the Li layer. However, at the Li saturation coverage, the intensity of diffraction spots at the Ir lattice positions [see Fig. 2(h)] increases due to the formation of (1 × 1) Li superstructure with respect to the Ir surface. We refer to this structure as Gr/Li(1 × 1)/Ir(111). At this level of Li concentration S_1 clearly hybridizes with the graphene π band thereby opening the energy band gap of 0.25 eV [see Fig. 2(e), marked by an arrow]. The shift and hybridization effects are also seen from the photoemission spectrum taken across the K point along the Γ–K–M (k_y) direction [Fig. 2(i), bandgap marked by an arrow]. Observe that the S_1 loses most of its spectral intensity after hybridization with the graphene π band, creating a membrane shaped structure in the (E,k) space that is stretched within the Dirac cone. The experimental results shown in Fig. 2 convey two important messages: (i) Li binding to the Ir(111) surface in the Gr/Li/Ir(111) system does not remove the S_1 from the valence band spectrum, and (ii) the spectral intensity of the surface state around the K point is virtually unaffected by Li at all Li concentrations. Figure 2(j) shows the EDC of the S_1 state during the de-intercalation process providing further support to both claims. It is interesting to look at the relation between binding energies of the Dirac point and S_1 with increasing Li concentration.

Figure 3(a) shows how the Dirac point binding energy increases with the Li deposition time suggesting the change of the trend at $E_B^D \approx 1.3$ eV. At the same time from Fig. 3(b) one can see that the SS exhibits very small energy change until the Dirac point reaches the same energy, i.e., 1.3 eV. As more Li is added the Dirac point and the SS show the same energy dependence. This behavior of the SS can be understood in terms of (i) high density of states that require a substantial charge transfer (from Li) to induce any observable shift and (ii) pinning to the graphene π bands at $E_B^D \approx 1.3$ eV through the mutual hybridization which is manifested as a rigid shift of graphene's Dirac cone and Ir SS.

To explore in which way graphene is responsible for this unexpected reappearance of the S_1 we employed the DFT to calculate the Li interaction with the Ir(111) SS band. Figure 4(a) and 4(b) show the band structure of 0.75 ML Li/Ir(111), and the same system overlaid with graphene, respectively. To mimic the various coverages and the disordered nature of the Li layer in the submonolayer coverage range, we have used in the calculation a large 4 × 4 unit cell consisting of 16 graphene cells. The Ir surface state is seen as a nondispersing band around the K point indicated by the (orange) circle in Figs. 4(a) and 4(b). The coherence of the state is represented by the width of the corresponding spectral line for a selected value of the wave vector k. The band structure of Li/Ir(111) and Gr/Li/Ir(111) systems for Li coverages ranging between 0 and 1 ML is shown in the Supplemental Material [29]. In both systems Li induces a shift of the SS to higher binding energies as observed experimentally. Li on the bare Ir(111) evidently induces deterioration of SS coherence (visible as a smearing

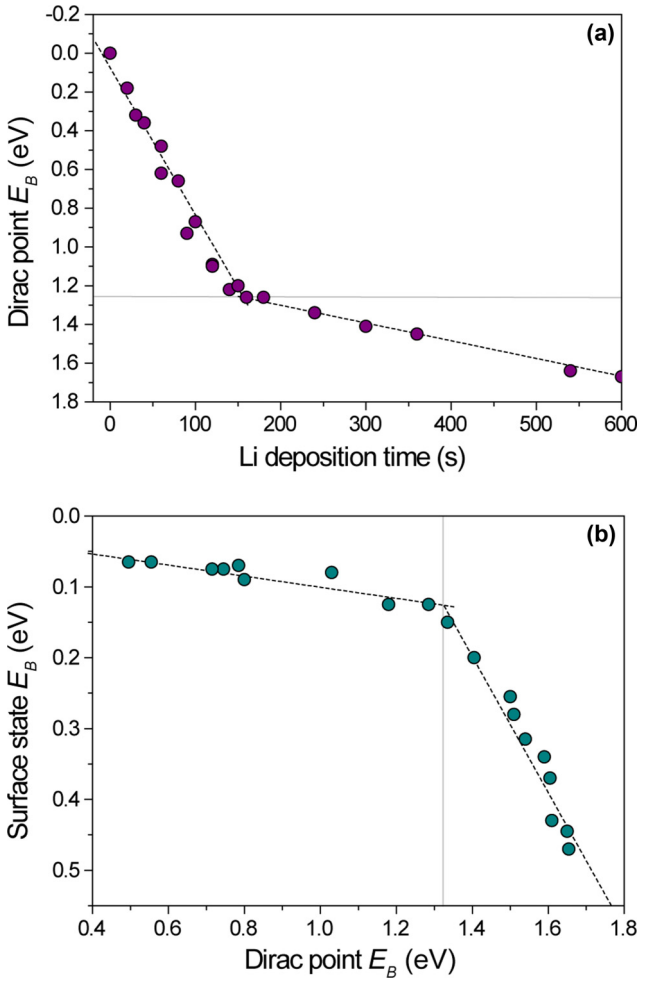

FIG. 3. (Color online) (a) Energy dependence of the Dirac point as a function of Li deposition time. (b) Binding energy of the Ir surface state as a function of Dirac point binding energy. The dashed lines correspond to the linear fits of the data appoints in the energy regions 1.3 eV $> E_B >$ 0 eV and 1.65 eV $> E_B >$ 1.3 eV.

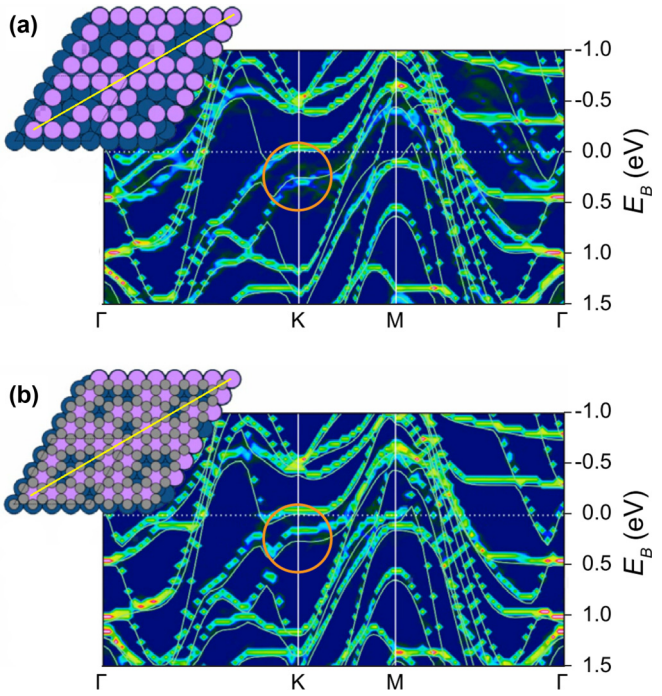

FIG. 4. (Color online) Calculated band structure of (a) Li/Ir(111) and (b) Gr/Li/Ir(111) for $\Theta = 0.75$ ML Li. The surface state around the *K* point, shifted to higher binding energies due to the interaction with Li is indicated by orange circle. Thin solid lines indicate the band structure of the Gr/Li(1 × 1)/Ir(111). Notice that the SS band feature [encircled in panel (a)] is smeared in energy when graphene is not present while in the case of Gr/Li/Ir(111) the SS feature is sharp [panel (b)].

of the flat line around *K*) with a caveat that when Li maximal coverage was calculated [corresponding to the ordered phase Ir(111)-(1 × 1)Li] the SS coherence was recovered. However, neither the formation of the (1 × 1)Li superstructure nor the recovery of the surface state was observed in the experiment. This clearly suggests that the electronic states of the disordered Li phase strongly contribute to the Ir SS decoherence as expected [33,34]. However, what is surprising is that same disordered phase of Li in the presence of graphene has no effect on the coherence of the Ir SS around the *K* point.

To understand possible channels through which this SS decoherence takes place and conversely, the mechanism through which graphene alters them, we calculated the charge transfer and the corresponding change of the density of states (DOS) induced by Li atoms. Figures 5(a) and 5(b) show a side view of the charge transfer density maps for 0.75 ML of Li on bare Ir(111) and Gr/Ir(111), respectively. In both maps there is a characteristic large amplitude of the charge rearrangement around the adsorbed (intercalated) Li. The calculations suggest that for Gr/Li/Ir(111) the charge originating from Li has been almost equally redistributed to the graphene and Ir surface layer (almost exclusively to the Ir surface state [29], in contrast to Cs intercalation where the charge is dominantly transferred to the Ir substrate [35]). Surprisingly, it appears as if the charge transferred from the Li to Ir surface does not depend on the presence of graphene. This is supported by the potential and DOS calculation shown in Fig. 5(c). The cross-section of the Gr/Li/Ir(111) structure has been superimposed by the corresponding potential and local DOS (LDOS) with and without graphene. The lower pair of curves in Fig. 5(c) shows the electronic potential perpendicular to the surface. Note that graphene bonded to the Ir(111) virtually does not influence the potential in the Ir surface layer. It is therefore not surprising that the charge transferred to the Ir surface layer is not visibly modified by the presence of graphene either [upper pair of curves in Fig. 5(c)]. Hence, it is puzzling how graphene imposes a difference in the behavior of the SS of Ir if the potential and the charge transferred from Li to the surface layer are not substantially altered by graphene itself. The answer to this question is sought in the charge redistribution in the (*E*,*k*) space. The presence of graphene offers to the Li/Ir(111) system a deep potential well that has a capacity to accept electrons within a wide phase space. Graphene redistributes these electrons across the energy spectrum thereby depleting Li DOS available for the interaction with Ir SS but increasing Li DOS at higher binding energies [see Fig. 5(d)]. The energy range around the Ir SS is expanded in Fig. 5(e) which shows LDOS projected on Li atoms for Li/Ir(111) and Gr/Li/Ir(111).

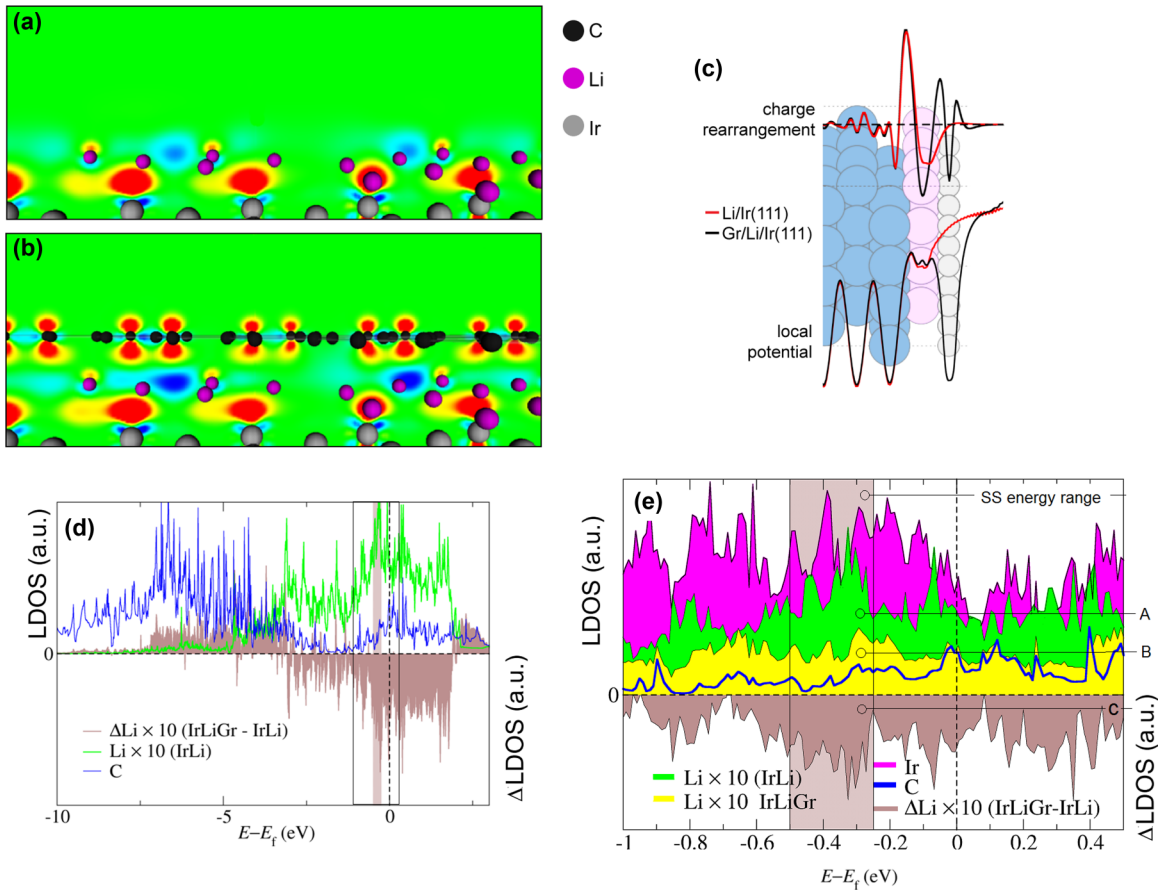

FIG. 5. (Color online) Charge transfer density maps of (a) Li/Ir(111) and (b) Gr/Li/Ir(111) for the Li coverage equal to 13/16 ML color coded in units of electron per $Å^3$ ranging from $0.02\,e/Å^3$ (red) and $-0.02\,e/Å^3$ (blue), taken along the directions indicated in Figs. 4(a) and 4(b). (c) Local potential (lower) and charge rearrangement (upper) curves corresponding to (a) red curve and (b) black curve structures. Both potential and charge difference along the z direction are averaged over the x-y planes. The charge difference is calculated as a difference between the system and freestanding system parts, i.e., for the case of Gr/Li/Ir $\frac{13}{16}$ it is δQ = charge(Gr/Li/Ir$\frac{13}{16}$) - charge(Ir surface) - charge (freestanding Li$\frac{13}{16}$) - charge(freestanding graphene). (d) LDOS projected on C atoms (blue) and Li atoms on Ir(111)(green). Brown area shows change of the LDOS projected on Li atoms upon graphene addition, indicating LDOS redistribution of Li states. (e) LDOS projected on Li atoms as indicated in the figure. Shaded area defines the energy range within which SS is dispersed around the K point, areas A and B correspond to the phase space available to SS electrons to scatter into Li states without and with graphene, respectively. C defines the reduction of the phase space available to SS electrons to scatter into Li states in the presence of graphene.

It is obvious that graphene significantly reduces LDOS on Li in the energy range corresponding to the Ir SS (shaded area). It is these Li states that are, through the mutual hybridization with the SS, responsible for its decoherence. Namely, the Ir surface state is characterized by the existence of a single wave function for every point in the phase space (E, k). The interaction of SS with the Li adsorbate introduces at particular k point of the SBZ additional wave functions associated with different electron energies. This interaction becomes a main channel for the incoherent scattering of Ir SS electrons which turns out to be efficiently blocked by graphene due to depletion of these Li states [see Fig. 5(e)].

A preservation of the SS for 1 ML Li [experimentally observed in Gr/Li/Ir(111) but not in Li/Ir(111)] can alternatively be explained as a consequence of the Li-ordered phase which follows perfectly the symmetry of the SS hence yielding a new coherent SS mixed with Li. Ir SS has been observed in Gr/Ir(111) intercalated by 1ML Cu [31] and Pt [32] systems. However, the lack of the data for Cu and Pt on bare Ir(111) and submonolayer Cu and Pt coverage in Gr/Cu/Ir(111) and Gr/Pt/Ir(111) systems prevents us from making any firm conclusion regarding the influence of graphene on the coherence of the SS for these two intercalants.

In conclusion, we demonstrated that the Ir SS which is strongly perturbed by the disordered Li overlayer recuperates its coherence around the K point when the system is overlaid with graphene. While the previous works on graphene intercalation have shown that intercalant can be efficiently used to separate graphene from the substrate, in this work we demonstrated how graphene participates in decoupling the intercalant from the substrate surface.

ACKNOWLEDGMENTS

P.P. and P.L thank B. Gumhalter and M. C. Asensio for fruitful discussions. We kindly acknowledge the experimental assistance of J. Avila at the ANTARES station of the SOLEIL

synchrotron. Financial support of the Croatian Science Foundation (IP-11-2013-2727) is acknowledged. I.Š.R. would like to thank the foundation L'Oréal: For Women in Science for financial support.

[1] W. Eberhardt, in *Synchrotron Radiat. Res. - Adv. Surf. Interface Sci.*, edited by R. Z. Bachrach, Vol. 1 (Plenum, New York, 1992).
[2] S. D. Kevan, Phys. Rev. B **28**, 2268 (1983).
[3] S. Å. Lindgren and L. Walldén, Solid State Commun. **34**, 671 (1980).
[4] F. Forster, A. Bendounan, J. Ziroff, and F. Reinert, Surf. Sci. **600**, 3870 (2006).
[5] H. Bentmann, A. Buchter, and F. Reinert, Phys. Rev. B **85**, 121412 (2012).
[6] S. D. Kevan, Surf. Sci. **178**, 229 (1986).
[7] V. Derycke, P. G. Soukiassian, F. Amy, Y. J. Chabal, M. D. D'angelo, H. B. Enriquez, and M. G. Silly, Nat. Mater. **2**, 253 (2003).
[8] S. M. Dounce, M. Yang, and H.-L. Dai, Surf. Sci. **565**, 27 (2004).
[9] A. Varykhalov, D. Marchenko, M. R. Scholz, E. D. L. Rienks, T. K. Kim, G. Bihlmayer, J. Sánchez-Barriga, and O. Rader, Phys. Rev. Lett. **108**, 066804 (2012).
[10] S. Ulstrup, M. Andersen, M. Bianchi, L. Barreto, B. Hammer, L. Hornekær, and P. Hofmann, 2D Mater. **1**, 025002 (2014).
[11] M. Kralj, I. Pletikosić, M. Petrović, P. Pervan, M. Milun, A. T. N'Diaye, C. Busse, T. Michely, J. Fujii, and I. Vobornik, Phys. Rev. B **84**, 075427 (2011).
[12] J. Klimeš, D. R. Bowler, and A. Michaelides, Phys. Rev. B **83**, 195131 (2011).
[13] H. J. Monkhorst and J. D. Pack, Phys. Rev. B **13**, 5188 (1976).
[14] G. Makov and M. C. Payne, Phys. Rev. B **51**, 4014 (1995).
[15] V. Popescu and A. Zunger, Phys. Rev. B **85**, 085201 (2012).
[16] P. V. C. Medeiros, S. Stafström, and J. Björk, Phys. Rev. B **89**, 041407 (2014).
[17] P. Lazić, N. Atodiresei, M. Alaei, V. Caciuc, S. Blügel, and R. Brako, Comput. Phys. Commun. **181**, 371 (2010).
[18] I. Pletikosić, M. Kralj, D. Sokčević, R. Brako, P. Lazić, and P. Pervan, J. Phys. Condens. Matter **22**, 135006 (2010).
[19] E. Starodub, A. Bostwick, L. Moreschini, S. Nie, F. El Gabaly, K. F. McCarty, and E. Rotenberg, Phys. Rev. B **83**, 125428 (2011).
[20] C. Virojanadara, S. Watcharinyanon, A. A. Zakharov, and L. I. Johansson, Phys. Rev. B **82**, 205402 (2010).
[21] L. Zhang, Y. Ye, D. Cheng, H. Pan, and J. Zhu, J. Phys. Chem. C **117**, 9259 (2013).
[22] E. Pollak, B. Geng, K.-J. Jeon, I. T. Lucas, T. J. Richardson, F. Wang, and R. Kostecki, Nano Lett. **10**, 3386 (2010).
[23] S. Watcharinyanon, L. I. Johansson, A. A. Zakharov, and C. Virojanadara, Surf. Sci. **606**, 401 (2012).
[24] F. Bisti, G. Profeta, H. Vita, M. Donarelli, F. Perrozzi, P. M. Sheverdyaeva, P. Moras, K. Horn, and L. Ottaviano, Phys. Rev. B **91**, 245411 (2015).
[25] T. P. Kaloni, Y. C. Cheng, M. Upadhyay Kahaly, and U. Schwingenschlögl, Chem. Phys. Lett. **534**, 29 (2012).
[26] M. A. Romero, A. Iglesias-García, and E. C. Goldberg, Phys. Rev. B **83**, 125411 (2011).
[27] G. Profeta, M. Calandra, and F. Mauri, Nat. Phys. **8**, 131 (2012).
[28] M. Andersen, L. Hornekær, and B. Hammer, Phys. Rev. B **90**, 155428 (2014).
[29] See Supplemental Material at http://link.aps.org/supplemental/10.1103/PhysRevB.92.245415 for additional information on (1) ARPES spectra of bare and Li intercalated Ir(111) (2) isosurfaces and the plane-cut plots of the eigenstates and (3) animated band structures, corresponding to Li/Ir and Gr/Li/Ir.
[30] A. V Fedorov, N. I. Verbitskiy, D. Haberer, C. Struzzi, L. Petaccia, D. Usachov, O. Y. Vilkov, D. V Vyalikh, J. Fink, M. Knupfer, B. Büchner, and A. Grüneis, Nat. Commun. **5**, 3257 (2014).
[31] H. Vita, S. Böttcher, K. Horn, E. N. Voloshina, R. E. Ovcharenko, T. Kampen, A. Thissen, and Y. S. Dedkov, Sci. Rep. **4**, 5704 (2014).
[32] I. I. Klimovskikh, O. Vilkov, D. Y. Usachov, A. G. Rybkin, S. S. Tsirkin, M. V. Filianina, K. Bokai, E. V. Chulkov, and A. M. Shikin, Phys. Rev. B **92**, 165402 (2015).
[33] K. Boger, T. Fauster, and M. Weinelt, New J. Phys. **7**, 110 (2005).
[34] B. Gumhalter, A. Šiber, H. Buljan, and T. Fauster, Phys. Rev. B **78**, 155410 (2008).
[35] M. Petrović, I. Šrut Rakić, S. Runte, C. Busse, J. T. Sadowski, P. Lazić, I. Pletikosić, Z.-H. Pan, M. Milun, P. Pervan, N. Atodiresei, R. Brako, D. Šokčević, T. Valla, T. Michely, and M. Kralj, Nat. Commun. **4**, 2772 (2013).